Research Article **Open Access**

Fabio Baronio*, Miguel Onorato, Shihua Chen, Stefano Trillo, Yuji Kodama, and Stefan Wabnitz

Optical-fluid dark line and X solitary waves in Kerr media

DOI 10.1515/odps-2017-0001
Received March 15, 2017; revised April 3, 2017; accepted April 10, 2017

Abstract: We consider the existence and propagation of nondiffractive and nondispersive spatiotemporal optical wavepackets in nonlinear Kerr media. We report analytically and confirm numerically the properties of spatiotemporal dark line solitary wave solutions of the $(2+1)D$ nonlinear Schrödinger equation (NLSE). Dark lines represent holes of light on a continuous wave background. Moreover, we consider nontrivial web patterns generated under interactions of dark line solitary waves, which give birth to dark X solitary waves. These solitary waves are derived by exploiting the connection between the NLSE and a well-known equation of hydrodynamics, namely the $(2+1)D$ type II Kadomtsev-Petviashvili (KP-II) equation. This finding opens a novel path for the excitation and control of optical solitary waves, of hydrodynamic nature.

Keywords: Nonlinear Optics; Self-action effects; Kerr effect; Solitons

***Corresponding Author: Fabio Baronio:** Istituto Nazionale di Ottica, CNR, and Dipartimento di Ingegneria dell'Informazione, Università di Brescia, Via Branze 38, 25123 Brescia, Italy, E-mail: fabio.baronio@unibs.it
Miguel Onorato: Dipartimento di Fisica, Università di Torino, Via P. Giuria 1, 10125 Torino, Italy, and Istituto Nazionale di Fisica Nucleare, INFN, Sezione di Torino, 10125 Torino, Italy
Shihua Chen: Department of Physics, Southeast University, Nanjing 211189, China
Stefano Trillo: Dipartimento di Ingegneria, Università di Ferrara, Via Saragat 1, 44122 Ferrara, Italy
Yuji Kodama: Department of Mathematics, Ohio State University, Columbus, OH 43210, USA
Stefan Wabnitz: Istituto Nazionale di Ottica, CNR, and Dipartimento di Ingegneria dell'Informazione, Università di Brescia, Via Branze 38, 25123 Brescia, Italy

1 Introduction

The propagation of high-intensity, ultra-narrow and ultra-short light pulses in quadratic and cubic nonlinear media is a complex multidimensional phenomenon which leads to substantial spatiotemporal pulse rearrangement. The spatiotemporal dynamics is influenced by the interaction of various physical effects, in particular diffraction, material dispersion and nonlinear response. This problem has attracted strong interest over the past decades, leading to the generation and the manipulation of high-intensity femtosecond and attosecond pulses [1, 2].

During the 1990s, extensive research activities concerning the self-focusing behavior of intense ultra-short pulses have shown that the spatial and temporal degrees of freedom have to be considered together [3–13]. When the effects of diffraction, dispersion and nonlinearity become comparable, the most fascinating result of space-time coupling is the possibility to form light bullets or spatiotemporal solitons. A strict constraint for the excitation of spatiotemporal solitons is that the nonlinear phase changes balance both the spatial front curvature and the dispersion-induced chirp, leading to spatiotemporal focusing. A anomalous dispersion enables the possibility to achieve bullet-type localized waves, while a normal dispersion rules out this possibility, while induces different behaviors such as temporal splitting and breaking.

During the 2000s, theoretical and experimental research activities have demonstrated that localized distortionless (both nondiffractive and nondispersive) wave packets also exist with normal dispersion in the form of X-wave solitons [14–16].

Counteracting the natural spatiotemporal spreading of wave packets is a universal and stimulating task, appearing in many fields of science and applied research, such as communications, optical data storage, spectroscopy, material processing, Bose-Einstein condensation, medical diagnostics, to name a few.

In this paper, we consider analytically and confirm numerically the existence and propagation of nondiffractive and nondispersive spatiotemporal solitons in self-

© 2017 Fabio Baronio et al., published by De Gruyter Open.
This work is licensed under the Creative Commons Attribution-NonCommercial-NoDerivs 3.0 License.

Unauthenticated
Download Date | 9/24/17 12:34 AM

focusing and normal dispersion Kerr media. At first, we show the existence and properties of dark line solitary waves of the $(2+1)D$ nonlinear Schrödinger equation (NLSE), which governs the propagation in self-focusing with normal dispersion. Then, we consider nontrivial web patterns generated under interactions of line solitons, which give birth to dark X solitary waves. The analytical dark solitary solutions are derived by exploiting the connection between the $(2+1)D$ NLSE and the $(2+1)D$ Kadomtsev-Petviashvili (KP) equation [17], a well-known equation of hydrodynamics. The latter constitutes the natural extension of the well-known (1+1)D Korteweg-de Vries (KdV) equation and it is widely employed in plasma physics and hydrodynamics (see e.g.[17–21]) in its two different forms, the so-called KP-I type and KP-II type, depending on the sign of the transverse perturbation to the KdV equation.

Our results extend and confirm the connection between nonlinear wave propagation in optics and hydrodynamics, that was established in the 1990's [22–27] and recently extensively studied [28, 29].

2 Theoretical Procedures

The dimensionless time-dependent paraxial wave equation in Kerr media, in the presence of group-velocity dispersion, and by limiting diffraction to one dimension, reads as [28]:

$$iu_z + \frac{\alpha}{2}u_{tt} + \frac{\beta}{2}u_{yy} + \gamma|u|^2u = 0, \tag{1}$$

where $u(t, y, z)$ represents the complex wave envelope; t, y represent temporal and spatial transverse coordinates, respectively, and z is the longitudinal propagation coordinate. Each subscripted variable in Eq. (1) stands for partial differentiation. α, β, γ are real constants that represent the effect of dispersion, diffraction and Kerr nonlinearity, respectively. We refer to Eq. (1) as *elliptic* NLSE if $\alpha\beta > 0$, and *hyperbolic* NLSE if $\alpha\beta < 0$. Of course, Eq. (1) may also describe (2+1)D spatial dynamics in cubic Kerr media, neglecting group-velocity dispersion; in this case t, y represent the spatial transverse coordinates, and z the longitudinal propagation coordinate; moreover $\alpha = \beta > 0$.

Writing $u = \sqrt{\rho}\exp(i\theta)$, and substituting in Eq. (1), we obtain for the imaginary and real parts of the field the following system of equations for (ρ, θ),

$$\begin{aligned}
&\rho_z + \alpha(\rho\theta_t)_t + \beta(\rho\theta_y)_y = 0,\\
&\theta_z - \gamma\rho + \frac{\alpha}{2}\left(\theta_t^2 + \frac{1}{4\rho^2}\rho_t^2 - \frac{1}{2\rho}\rho_{tt}\right) +\\
&\quad + \frac{\beta}{2}\left(\theta_y^2 + \frac{1}{4\rho^2}\rho_y^2 - \frac{1}{2\rho}\rho_{yy}\right) = 0.
\end{aligned} \tag{2}$$

Let us consider now small corrections to the stationary continuous wave (cw) background solutions of Eqs. (2), and set

$$\rho = \rho_0 + \epsilon\rho_1, \qquad \theta = \theta_0 + \epsilon\theta_1 \tag{3}$$

with ρ_0 constant, $\theta_0 = \gamma\rho_0 z$. ϵ is a small positive extension parameter ($0 < \epsilon \ll 1$). We introduce the variables $\eta = \epsilon\rho_1$ and $\phi = \epsilon\theta_1$ and assume the following scalings $\eta \sim \phi_z \sim \phi_t \sim \mathcal{O}(\epsilon)$, $\partial_t \sim \partial_z \sim \mathcal{O}(\epsilon^{1/2})$, $\partial_y \sim \mathcal{O}(\epsilon)$. Then we obtain from Eqs. (2)

$$\begin{aligned}
&\eta_z + \rho_0(\alpha\phi_{tt} + \beta\phi_{yy}) + \alpha(\eta\phi_t)_t = \mathcal{O}(\epsilon^{7/2}),\\
&\phi_z - \gamma\eta + \frac{\alpha}{2}\left(\phi_t^2 - \frac{1}{2\rho_0}\eta_{tt}\right) = \mathcal{O}(\epsilon^3).
\end{aligned} \tag{4}$$

Introducing the coordinates $\tau = t - c_0 z$, $\upsilon = y$, $\varsigma = z$ ($c_0 = \sqrt{-\gamma\alpha\rho_0}$), and noting that $\partial_\varsigma \sim \mathcal{O}(\epsilon^{3/2})$, from Eqs. (4) we have

$$\begin{aligned}
&-c_0\eta_\tau + \eta_\varsigma + \rho_0\alpha\phi_{\tau\tau} + \rho_0\beta\phi_{\upsilon\upsilon} + \alpha(\eta\phi_\tau)_\tau = \mathcal{O}(\epsilon^{7/2})\\
&-c_0\phi_\tau + \phi_\varsigma - \gamma\eta + \frac{\alpha}{2}\left(\phi_\tau^2 - \frac{1}{2\rho_0}\eta_{\tau\tau}\right) = \mathcal{O}(\epsilon^3).
\end{aligned} \tag{5}$$

From the second of Eqs. (5), we obtain $\eta = -\frac{c_0}{\gamma}\phi_\tau +$ *(higher order terms)*; iterating to find the higher order terms, we obtain

$$\eta = \frac{1}{\gamma}\left(-c_0\phi_\tau + \phi_\varsigma + \frac{\alpha}{2}\phi_\tau^2 - \frac{\alpha^2}{4c_0}\phi_{\tau\tau\tau}\right) + \mathcal{O}(\epsilon^3). \tag{6}$$

By inserting (6) in the first of Eqs. (5), we have

$$\phi_{\tau\varsigma} + \frac{3\alpha}{4}(\phi_\tau^2)_\tau - \frac{\alpha^2}{8c_0}\phi_{\tau\tau\tau\tau} + \frac{c_0\beta}{2\alpha}\phi_{\upsilon\upsilon} = \mathcal{O}(\epsilon^3). \tag{7}$$

Eq. (7) is known as the potential KP equation [20]. In fact, from Eq. (7) we obtain the evolution equation for η, namely, we have the KP equation at the leading order,

$$\left(-\eta_\varsigma + \frac{3\alpha\gamma}{2c_0}\eta\eta_\tau + \frac{\alpha^2}{8c_0}\eta_{\tau\tau\tau}\right)_\tau - \frac{c_0\beta}{2\alpha}\eta_{\upsilon\upsilon} = 0. \tag{8}$$

Notice that, in the case $\alpha > 0$, $\beta > 0$, $\gamma < 0$, we have the KP-I type, and when $\alpha < 0$, $\gamma > 0$, $\beta > 0$, the KP-II type.

Therefore, we underline that the optical NLSE solution $u(t, y, z)$ of hydrodynamic KP origin $[\eta(\tau, \upsilon, \varsigma), \phi(\tau, \upsilon, \varsigma)]$ can be written as [28, 29]:

$$u(t, y, z) = \sqrt{\rho_0 + \eta(\tau, \upsilon, \varsigma)}\; e^{i(\gamma\rho_0 z + \phi(\tau, \upsilon, \varsigma))}, \tag{9}$$

Unauthenticated
Download Date | 9/24/17 12:34 AM

with $\phi = -(\gamma/c_0)\int_\tau \eta$, $\tau = t - c_0 z$, $\upsilon = y$ and $\varsigma = z$.

Of interest in the optical context, the *elliptic* anomalous dispersion and self-defocusing regime ($\alpha > 0, \beta > 0, \gamma < 0$) leads to the KP-I regime, while the *hyperbolic* normal dispersion and self-focusing regime ($\alpha < 0, \gamma > 0, \beta > 0$) leads to the KP-II regime. Without loss of generality, we may set the following constraints to the coefficients of Eq. (1), $|\alpha| = 4\sqrt{2}, \beta = 6\sqrt{2}, |\gamma| = 2\sqrt{2}$; moreover, we fix $\rho_0 = 1$ (thus $c_0 = 4$). Note that, with the previous relations among its coefficients, in the case ($\alpha > 0$, $\beta > 0, \gamma < 0$) the Eq. (8) reduces to the standard KP-I form: $(-\eta_\varsigma - 6\eta\eta_\tau + \eta_{\tau\tau\tau})_\tau - 3\eta_{\upsilon\upsilon} = 0$; in the case ($\alpha < 0$, $\gamma > 0, \beta > 0$) the Eq. (8) reduces to the standard KP-II form $(-\eta_\varsigma - 6\eta\eta_\tau + \eta_{\tau\tau\tau})_\tau + 3\eta_{\upsilon\upsilon} = 0$.

3 Results and Discussion

Here, we focus our attention on the combined action of diffraction and normal dispersion for self-focusing media, thus we consider the optical NLSE–hydrodynamic KP-II correspondence. The results that we derive below have relevance also for different contexts where the same hyperbolic NLSE applies, such as the propagation in suitably engineered lattices giving rise to effective negative diffraction [30, 31] (in this case t represents in Eq. (1) an additional spatial variable).

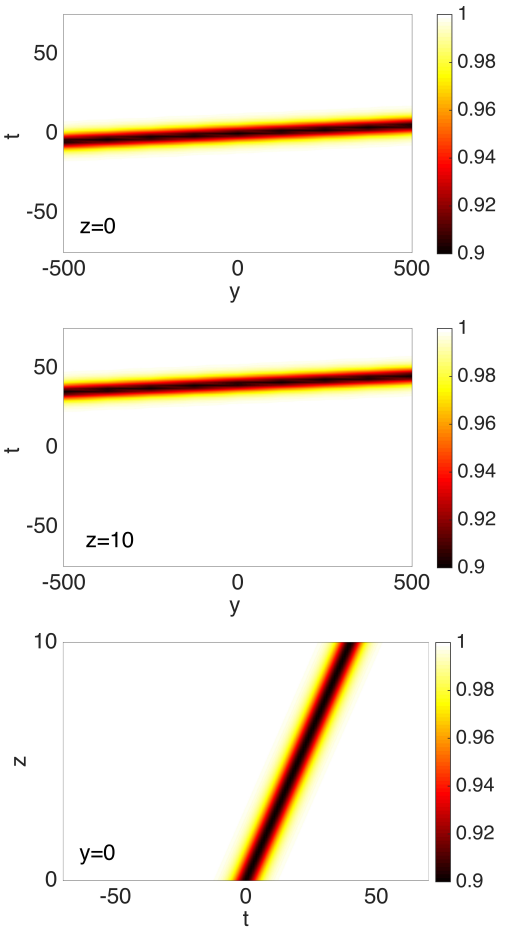

Figure 1: Analytical spatiotemporal dark-lump NLSE envelope intensity distribution $|u(t, y, z)|^2$, shown in the $y - t$ plane, at $z = 0$, at $z = 10$, and in the $t - z$ plane at $y = 0$. Here, $\epsilon = 0.1$, $\varphi = 0.01$.

3.1 NLSE dark line solitary wave propagation

At first, we proceed to consider the existence and propagation of $(2 + 1)D$ NLSE dark line solitary waves, which are predicted by the existence of $(2+1)D$ KP bright line solitons [20, 21]. When considering the small amplitude regime, a formula for an exact line bright soliton of Eq. (8) can be expressed as follows [20]:

$$\eta(\tau, \upsilon, \varsigma) = -\epsilon\ sech^2[\sqrt{\epsilon/2}(\tau + tan\varphi\ \upsilon + c\varsigma)], \qquad (10)$$

where ϵ rules the amplitude and width of the soliton, φ is the angle measured from the υ axis in the counterclockwise, $c = 2\epsilon + 3tan^2\varphi$ is the velocity in τ-direction. Notice that c is of order ϵ. Moreover we obtain $\phi(\tau, \upsilon, \varsigma) = \sqrt{\epsilon}\ tanh([\sqrt{\epsilon/2}(\tau + tan\varphi\ \upsilon + c\varsigma)]$.

Figure 1 shows the analytical spatiotemporal envelope intensity profile $|u(t, y, z)|^2 = 1+\eta(\tau = t-c_0 z, \upsilon = y, \varsigma = z)$ of a NLSE dark line solitary wave, given by the mapping (9) exploiting the KP bright soliton expression (10), in the $y - t$ plane at $z = 0$, at $z = 10$, and in the $t - z$ plane at $y = 0$, for $\epsilon = 0.1$ and $\varphi = 0.01$. The intensity dip of the dark line solitary wave is $-\epsilon$, the velocity $c_0 - c - 3tan^2\varphi = 4 - 2\epsilon - 3tan^2\varphi$ in the z-direction.

Next, we numerically verified the accuracy of the analytically predicted dark line solitary waves of the NLSE. To this end, we made use of a standard split-step Fourier technique, commonly adopted in the numerical solution of the NLSE (1). We take the dark wave envelope at $z = 0$ as the numerical input: $u(t, y, z = 0) = \sqrt{1 + \eta(\tau = t, \upsilon = y, \varsigma = 0)}\exp\left[i\phi(\tau = t, \upsilon = y, \varsigma = 0)\right]$, where η is the line-soliton solution (10). Figure 2 shows the numerical spatiotemporal envelope intensity profile $|u(t, y, z)|^2$ of a NLSE dark line solitary wave, which corresponds to the analytical dynamics reported in Fig. 1.

As can be seen from the images included in Figs. 1–2 the numerical solutions of the NLSE show an excellent agreement with the analytical approximate NLSE solitary solutions. Only a small low amplitude radiative emis-

Unauthenticated
Download Date | 9/24/17 12:34 AM

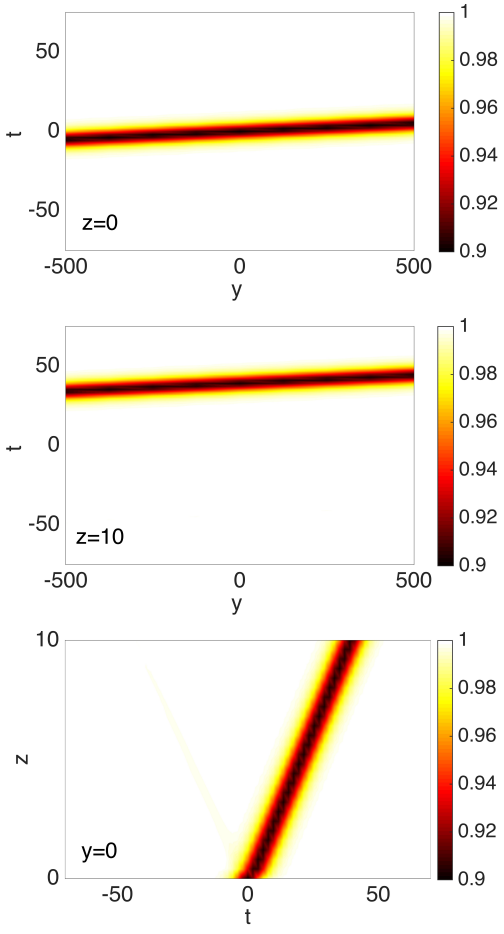

Figure 2: Numerical spatio-temporal dark-lump NLSE envelope intensity distribution $|u(t, y, z)|^2$, shown in the $y - t$ plane, at $z = 0$, at $z = 10$ and in the $t - z$ plane at $y = 0$. Here, $\epsilon = 0.1$, $\varphi = 0.01$.

sion can be detected at the beginning of propagation. The NLSE–KP mapping works well also for higher value of ϵ. We considered the effective energy $\overline{E}$ of envelope u:

$$\overline{E} = \int\int (|u|^2 - \rho_0) dt\, dy,$$

and we defined the relative error function $e = (\overline{E} - \overline{E}_{exact})/\overline{E}_{exact}$, where $\overline{E}$ represents the numerical effective energy of the excited dark solitary wave and $\overline{E}_{exact}$ is the effective energy of the solitary solution of KP-II origin. Figure 3 reports the error function e [%] as a function of ϵ. Notice that $\epsilon = 1$ is the maximum allowed value, since $\rho_0 = 1$, which gives a black dark solitary wave.

3.2 NLSE dark X solitary wave propagation

In the long wave context, the KP-II equation admits complex soliton solutions, mostly discovered and demonstrated in the last decade [20, 21], which may describe nontrivial web patterns generated under resonances of line-solitons.

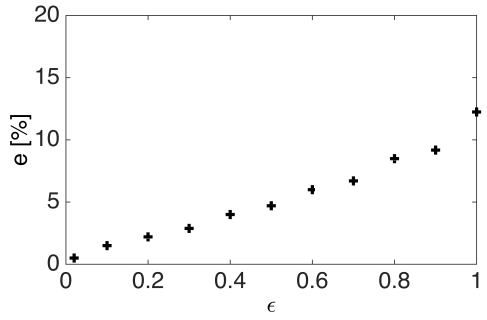

Figure 3: Error function e [%] versus ϵ values. Here, $\varphi = 0$.

Here, we consider the resonances of four line solitons, which give birth to the so-called *O-type* bright X-shaped two-soliton solution of the KP-II (the name *O-type* is due to the fact that this solution was *originally* found by using the Hirota bilinear method [20]). When considering the small amplitude regime, the formula of the *O-type* solution of Eq. (8) can be expressed as follows [20],

$$\eta(\tau, \upsilon, \varsigma) = -2\,(\ln F)_{\tau\tau}\,, \tag{11}$$

where the function $F(\tau, \upsilon, \varsigma)$ is given by $F = f_1 + f_2$ with

$$f_1 = (\epsilon_1 + \epsilon_2)\cosh[(\epsilon_1 - \epsilon_2)\tau + 4\,(\epsilon_1^3 - \epsilon_2^3)\varsigma]$$
$$f_2 = 2\sqrt{\epsilon_1\epsilon_2}\cosh[(\epsilon_1^2 - \epsilon_2^2)\upsilon].$$

ϵ_1, ϵ_2 are small real positive parameters which are related to the amplitude, width and the angle of the *O-type* X-soliton solutions.

The corresponding (2+1)D NLSE dark X solitary wave $u(t, y, z)$, is directly given through the mapping Eq. (9), by exploiting the soliton expression for $\eta(\tau, \upsilon, \varsigma)$ in Eq. (11).

Figure 4 shows the spatiotemporal envelope intensity profile $|u(t, y, z)|^2 = 1 + \eta(\tau = t - c_o z, \upsilon = y, \varsigma = z)$ of a (2+1)D NLSE dark X solitary wave of the hyperbolic NLSE. The solution is shown in the (y, t) plane, at $z = 0$ and at $z = 10$. In this particular example we have chosen $\epsilon_1 = 0.2$, $\epsilon_2 = 0.001$. Specifically, Fig. 4 illustrates a solitary solution which describes the X-interaction of four dark line solitons. The maximum value of the dip in the interaction region is $2(\epsilon_1 - \epsilon_2)^2\,(\epsilon_1 + \epsilon_2)/(\epsilon_1 + \epsilon_2 + 2\sqrt{\epsilon_1\epsilon_2})$. Asymptotically, the solution reduces to two line dark waves for $t \ll 0$ and two for $t \gg 0$, with intensity dips $\frac{1}{2}(\epsilon_1 - \epsilon_2)^2$ and characteristic angles $\pm\tan^{-1}(\epsilon_1 + \epsilon_2)$, measured from the y axis. Next, we numerically verified the accuracy of the analytically predicted *O-type* dark X solitary wave of

Unauthenticated
Download Date | 9/24/17 12:34 AM

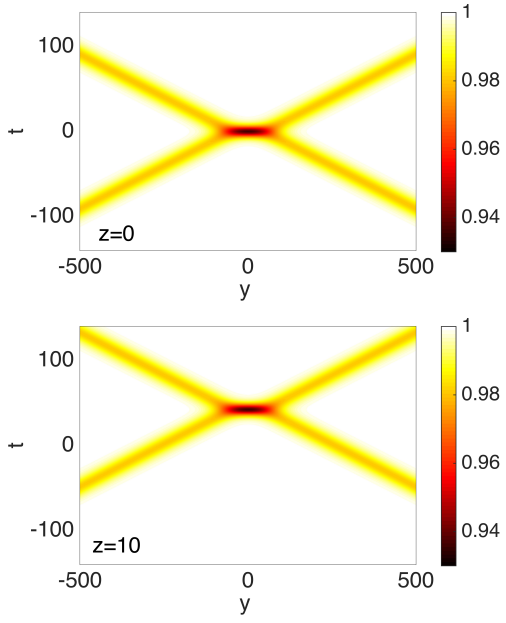

Figure 4: Analytical spatiotemporal NLSE envelope intensity distribution $|u(t, y, z)|^2$, in the (y, t) plane, showing the dark X solitary wave dynamics, at $z = 0$ and at $z = 10$. Here, $\epsilon_1 = 0.2$, $\epsilon_2 = 0.001$.

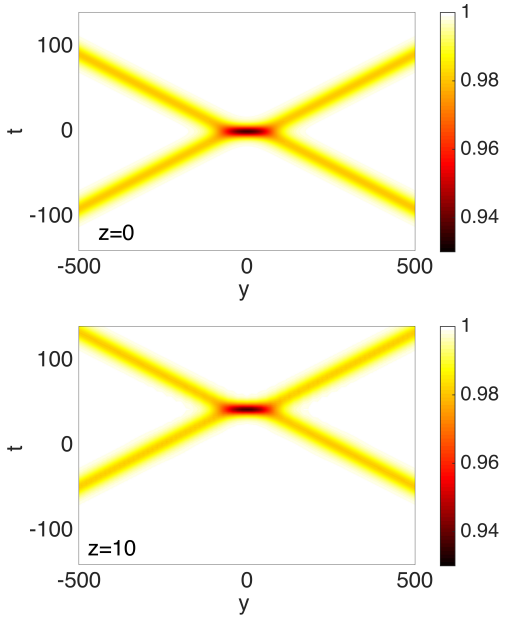

Figure 5: Numerical spatiotemporal NLSE envelope intensity distribution $|u(t, y, z)|^2$, in the (y, t) plane, showing the dark X solitary wave dynamics, at $z = 0$ and at $z = 10$. Here, $\epsilon_1 = 0.2$, $\epsilon_2 = 0.001$.

the NLSE. As done previously, we took the dark wave envelope at $z = 0$ as the numerical input: $u(t, y, z = 0) = \sqrt{1 + \eta(\tau = t, \upsilon = y, \varsigma = 0)} \exp\left[i\phi(\tau = t, \upsilon = y, \varsigma = 0)\right]$, where η is the X-soliton solution (11). Fig. 5 shows the (y, t) profile of the numerical solution of the hyperbolic NLSE at $z = 0$, and at $z = 10$. Numerical simulations and analytical predictions are in excellent agreement. We estimate the error between the asymptotic formula and the X solitary wave in the numerics to be lower than 2%.

The proposed solutions propagate as X-shaped nonlinear invariant modes of the NLSE, being subject only to a net delay due to the velocity c. The spatio-temporal Fourier spectrum of these waves is also X-shaped (see Fig. 6). These features allow us to classify such modes in the huge class of diffraction-free and dispersion-free X waves. We emphasize, however, that there are differences with respect to the more general nonlinear X wave solutions reported in the literature for the (3+1)D hyperbolic NLSE [14, 32]. In particular, the latter type of X waves exhibit a characteristic decay $1/r$ along the spatial coordinate r which is characteristic of Bessel functions constituting the building blocks of X waves in the linear propagation regime. Conversely, in the present case, the dark X solitary waves have constant asymptotic, the line solitons. Nevertheless, the asymptotic state is compatible with 1D transverse diffraction, a regime where the connections between the linear and nonlinear X-waves have not been exhaustively investigated yet.

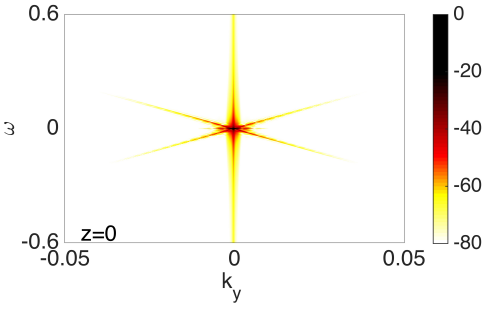

Figure 6: Normalized (dB) spatiotemporal NLSE envelope intensity distribution in the (k_y, ω) plane, at $z = 0$ of the dark X solitary wave reported in Figs. 4-5.

Overall, these results provide a clear evidence that theoretical and experimental phenomenologies of the hydrodynamic shallow water X waves dynamics can be mapped into the realm of multidimensional spatiotemporal nonlinear optics.

Unauthenticated
Download Date | 9/24/17 12:34 AM

3.3 Instabilities

Let us finally discuss the important issue of the stability of the predicted dark line and X solitary waves of the hyperbolic NLSE. Two instability factors may affect the propagation of these waves. The first one is the modulation instability (MI) of the continuous wave background. In the case considered here ($\alpha < 0$, $\beta, \gamma > 0$) MI is of the conical type [33–35]. Generally speaking, MI can be advantageous to form X waves from completely different initial conditions both in the absence [14] or in the presence [36] of the background. The second mechanism is related to the transverse instability of the line solitons that compose the asymptotic state of the X wave [37]. We point out that such instability is known to occur for the NLSE despite the fact that line solitons are transversally stable in the framework of the KP-II (unlike those of the KP-I) [17]. However, in our simulations of the NLSE, these transverse instabilities never appears, since they are extremely long range especially for shallow solitons.

In fact, we found that the primary mechanism that affects the stability of dark line and X solitary waves is the MI of the background. As a result the onset of MI causes the distortion of the solitary waves due to the amplification of spatiotemporal frequencies which are outside the spatiotemporal soliton spectrum. However, typically this occurs only after tens of nonlinear lengths, usually beyond the sample lengths employed in optical experiments. Indeed, the effect of MI becomes visible only for distances longer than those shown in Figs. 1-2, i.e. for $z > 10 - 20$.

4 Conclusions

We have analytically predicted and numerically validated a class of dark line solitary wave solutions that describes nondiffractive and nondispersive spatiotemporal localized wave packets propagating in optical Kerr media, in the self-focusing and normal dispersion regime. Moreover, we have reported non-trivial web patterns made of dark line solitary waves, which generate X dark solitary waves, of hydrodynamic essence. The key property of these solutions is that their existence and interactions are inherited from the hydrodynamic soliton solutions of the well-known KP-II equation.

This finding opens a novel path for the excitation and manipulation of line and X waves in nonlinear optics and in other areas where the NLSE applies, from Bose-Einstein condensation to acoustics. In fact, the nonlinear dark line and X solitary wave solutions of the NLSE are potentially observable in the regimes investigated experimentally in [15, 16, 31] and also in [10, 13, 38, 39]. Of course any finite energy realization of the present type of solutions should consider a spatiotemporal envelope modulation of the X solitary wave that decays to zero sufficiently slowly in (t, y) when compared with the extension of the solitary central notch, similarly to the case of dark solitons in $(1+1)D$ [40] and $(2+1)D$ [41].

Acknowledgement: The present research was partially supported by the Italian Ministry of University and Research (MIUR) (2012BFNWZ2), and has received funding from the European Union's Horizon 2020 research and innovation programme under the Marie Sklodowska-Curie grant agreement No 691051.

References

[1] R. Boyd, *Nonlinear Optics*, 3rd ed. (Academic Press, London, 2008).
[2] A. Weiner, *Ultrafast Optics* (Wiley, New York, 2009).
[3] Y. Silberberg, Collapse of optical pulses, Opt. Lett. **15**, 1282 (1990).
[4] J. E. Rothenberg, Pulse splitting during self-focusing in normally dispersive media, Opt. Lett. **17**, 583 (1992).
[5] J. K. Ranka, R. W. Schirmer, and A. L. Gaeta, Observation of pulse splitting in nonlinear dispersive media, Phys. Rev. Lett. **77**, 3783 (1996).
[6] J. R. Ranka and A. L. Gaeta, Breakdown of the slowly varying envelope approximation in the self-focusing of ultrashort pulses, Opt. Lett. **23**, 534 (1998).
[7] A. A. Zozulya, S. A. Diddams, A. G. Van Egen, and T. S. Clement, Propagation Dynamics of Intense Femtosecond Pulses: Multiple Splittings, Coalescence, and Continuum Generation, Phys. Rev. Lett. **82**, 1430 (1999).
[8] X. Liu, L. J. Qian, and F.W. Wise, Generation of Optical Spatiotemporal Solitons, Phys. Rev. Lett. **82**, 4631 (1999).
[9] I.G. Koprinkov, A. Suda, P. Wang, and K. Midorikawa, Self-Compression of High-Intensity Femtosecond Optical Pulses and Spatiotemporal Soliton Generation, Phys. Rev. Lett. **84**, 3847 (2000).
[10] H. S. Eisenberg, R. Morandotti, Y. Silberberg, S. Bar-Ad, D. Ross, and J. S. Aitchison, Kerr Spatiotemporal Self-Focusing in a Planar Glass Waveguide, Phys. Rev. Lett. **87**, 043902 (2001).
[11] S. Tzortzakis, L. Sudrie, M. Franco, B. Prade, and M. Mysyrowicz, A. Couairon, and L. Bergé, Kerr Spatiotemporal Self-Focusing in a Planar Glass Waveguide, Phys. Rev. Lett. **87**, 043902 (2001).
[12] P.H. Pioger, V. Couderc, L. Lefort, A. Barthelemy, F. Baronio, C. De Angelis, Spatial trapping of short pulses in Ti-indiffused LiNbO3 waveguides, Y. Min, V. Quiring, and W. Sohler, Opt. Lett. **27**, 2182 (2002).
[13] F. Baronio, C. De Angelis, P.H. Pioger, V. Couderc, and A. Barthelemy, Reflection of quadratic solitons at the boundary of nonlinear media, Opt. Lett. **29**, 986 (2004).

Unauthenticated
Download Date | 9/24/17 12:34 AM

[14] C. Conti, S. Trillo, P. Di Trapani, G. Valiulis, A. Piskarskas, O. Jedrkiewicx, and J. Trull, Nonlinear Electromagnetic X Waves, Phys. Rev. Lett. **90**, 170406 (2003).
[15] P. Di Trapani, G. Valiulis, A. Piskarskas, O. Jedrkiewicx, J. Trull, C. Conti, and S. Trillo, Spontaneously Generated X-Shaped Light Bullets, Phys. Rev. Lett. **91**, 093904 (2003).
[16] O. Jedrkiewicz, A. Picozzi, M. Clerici, D. Faccio, and P. Di Trapani, Emergence of X-Shaped Spatiotemporal Coherence in Optical Waves, Phys. Rev. Lett. **97**, 243903 (2006).
[17] B.B. Kadomtsev and V.I. Petviashvili, On the stability of solitary waves in weakly dispersing media, Sov. Phys. - Dokl. **15**, 539 (1970).
[18] J. Miles, Obliquely interacting solitary waves, J. Fluid Mech. **79**, 157 (1977);
[19] M. J. Ablowitz and H. Segur, *Solitons and the inverse scattering transform*, SIAM Stud. in Appl. Math. (SIAM, Philadelphia, 1981).
[20] Y. Kodama, KP Solitons in shallow water, J. Phys. A: Math. Theor. **43**, 434004 (2010).
[21] W. Li, H. Yeh and Y. Kodama, On the Mach reflection of a solitary wave: revisited, J. Fluid Mech. **672**, 326 (2011).
[22] E.A. Kuznetsov and S.K. Turitsyn, Instability and collapse of solitons in media with a defocusing nonlinearity, Sov. Phys. JEPT **67**, 1583 (1988).
[23] G.A. Swartzlander and C.T. Law, Optical vortex solitons observed in Kerr nonlinear media, Phys. Rev. Lett. **69**, 2503 (1992).
[24] D.E. Pelinovsky, Y.A. Stepanyants, Y.S. Kivshar, Self-focusing of plane dark solitons in nonlinear defocusing media, Phys. Rev. E **51**, 5016 (1995).
[25] V. Tikhonenko, J. Christou, B. Luther-Davies, and Y. S. Kivshar, Observation of vortex solitons created by the instability of dark soliton stripes, Opt. Lett. **21**, 1129 (1996).
[26] D.J. Frantzeskakis, K. Hizanidis, B.A. Malomed, and C. Polymilis, Stable anti-dark light bullets supported by the third-order dispersion, Phys. Lett. A **248**, 203 (1998).
[27] Y. Kodama and S. Wabnitz, Analytical theory of guiding-center nonreturn-to-zero and return-to-zero signal transmission in normally dispersive nonlinear optical fibers, Opt. Lett. **20**, 2291 (1995).
[28] F. Baronio, S. Wabnitz, and Y. Kodama, Optical Kerr spatiotemporal dark-lump dynamics of hydrodynamic origin, Phys. Rev. Lett. **116**, 173901 (2016).
[29] F. Baronio, S. Chen, M. Onorato, S. Trillo, S. Wabnitz, and Y. Kodama, Spatiotemporal optical dark X solitary waves, Opt. Lett. **41**, 5571 (2016).
[30] H. S. Eisenberg, Y. Silberberg, R. Morandotti, and J. S. Aitchison, Diffraction Management, Phys. Rev. Lett. 85, 1863 (2000).
[31] Y. Lahini, E. Frumker, Y. Silberberg, S. Droulias, K. Hizanidis, R. Morandotti, and D. N. Christodoulides, Discrete X-Wave Formation in Nonlinear Waveguide Arrays, Phys. Rev. Lett. **98**, 023901 (2007).
[32] R. W. Boyd, S. G. Lukishova, Y. R. Shen, *Self-focusing: Past and Present, Fundamentals and Prospects*, (Springer, New York, 2009).
[33] H. C. Yuen and B. M. Lake, Instabilities of waves on deep-water, Ann. Rev. Fluid Mech. **12**, 303 (1980).
[34] P. K. Newton and J. B. Keller, Stability of periodic plane waves, SIAM J. Appl. Math. **47**, 959 (1987).
[35] G.G. Luther, A.C. Newell, J.V. Moloney, and E.M. Wright, Short-pulse conical emission and spectral broadening in normally dispersive media, Opt. Lett. **19**, 789 (1994).
[36] Y. Kominis, N. Moshonas, P. Papagiannis, K. Hizanidis, and D. N. Christodoulides, Continuous wave controlled nonlinear X-wave generation, Opt. Lett. **30**, 2924 (2005).
[37] K. Rypdal and J. J. Rasmussen, Stability of solitary structures in the nonlinear Schrödinger equation, Phys. Scripta **40**, 192 (1989).
[38] F. Baronio, C. De Angelis, M. Marangoni, C. Manzoni, R. Ramponi, and G. Cerullo, Spectral shift of femtosecond pulses in nonlinear quadratic PPSLT Crystals, Opt. Express **14**, 4774 (2006).
[39] K. Krupa, A. Labruyere, A. Tonello, B. M. Shalaby, V. Couderc, F. Baronio, and A. B. Aceves, Polychromatic filament in quadratic media: spatial and spectral shaping of light in crystals, Optica **2**, 1058 (2015).
[40] D. Krokel, N.J. Halas, G. Giuliani, and D. Grishkowsky, Dark pulse propagation in optical fibers, Phys. Rev. Lett. **60**, 29 (1988).
[41] F. Baronio, M. Conforti, C. De Angelis, A. Degasperis, M. Andreana, V.Couderc, and A. Barthelemy, Velocity-Locked Solitary Waves in Quadratic Media', Phys. Rev. Lett. **104**, 113902 (2010).

Unauthenticated
Download Date | 9/24/17 12:34 AM